A First-Principles Approach to Studying the Thermal Stability of Oxide Cathode Materials

L. Wang, T. Maxisch, and G. Ceder*

Department of Materials Science and Engineering, Massachusetts Institute of Technology, Cambridge, Massachusetts 02139

Received September 4, 2006. Revised Manuscript Received November 15, 2006

We present a new method for predicting the thermodynamics of thermal degradation of charged cathode materials for rechargeable Li batteries and demonstrate it on three cathode materials, Li_xNiO_2, Li_xCoO_2, and $Li_xMn_2O_4$. The decomposition of Li_xNiO_2 is a two-step process: the first step is a kinetically controlled exothermic conversion in which the layered structure transforms to the stable spinel structure. The second step is an endothermic decomposition of the spinel into a rocksalt phase, accompanied by the loss of oxygen. The heat generation for the overall reaction from the layered to the rocksalt structure is exothermic when $x < 0.5$ and endothermic when $x > 0.5$. From the calculated phase diagram, a similar mechanism is expected for Li_xCoO_2, but the high migration barrier for Co may inhibit the layered-to-spinel transformation and lead to decomposition into $LiCoO_2$ and Co_3O_4. For the stable spinel $LiMn_2O_4$, high temperature is needed to provide enough thermodynamic driving force for its endothermic decomposition reaction. The fully charged λ-Mn_2O_4 transforms kinetically into the stable phase β-MnO_2 first and then decomposes at elevated temperature into the lower-valence oxides, α-Mn_2O_3 and Mn_3O_4. The calculated decomposition heat for the three systems is in good agreement with experiments. When present, the electrolyte can act as a sink for the oxygen released from the cathode. Although oxygen release from the cathode is generally endothermic, its combustion with the electrolyte leads to a highly exothermic reaction.

1. Introduction

Safety issues are a serious concern for Li-ion cells. As more Li is electrochemically removed from the cathode in a drive for higher energy density, the electrode material becomes highly oxidized and may degrade through exothermic or endothermic phase transitions. The decomposition of the cathode material at a high state of charge can result in the release of heat and oxygen gas, which can lead to runaway reactions. To improve the thermal stability of rechargeable lithium batteries, it is important to understand the thermal degradation mechanisms of cathode materials at various charging states.

First-principles computations have been shown to be effective in predicting a wide variety of materials properties, including the intercalation voltage,[1] Li-vacancy ordering,[2] Li diffusion,[3,4] complex transition-metal ordering,[5] and recently, even electronic transport.[6] However, little or no computational studies on understanding the stability of cathode materials at the high state of charge have been reported. This problem is in part due to the difficulty of correctly predicting the energy of reduction reactions with density functional theory (DFT) when the local density approximation (LDA) or generalized gradient approximation (GGA) is used for the exchange-correlation correction.[7] This problem is particularly crucial when studying the thermal stability of cathodes as their decomposition is almost always driven by a tendency to reduce the highly charged electrode. It was recently shown that the self-interaction present in LDA and GGA, which is responsible for the underestimation of the redox potential,[8] also creates significant errors in the enthalpy of standard oxidation/reduction reaction.[7] The availability of practical LDA+U schemes, in which much of the self-interaction in transition metals due to correlation effects of the localized d or f electrons is removed,[9,10] opens up the possibility of quantitative investigations of cathode instabilities at highly charged states.

For a phase transformation of an electrode material to occur, a thermodynamic driving force toward another phase (or combination of phases) needs to exist. If the mobility of the ions is high enough to allow their migration at the temperature at which the free energy change for the conversion is negative, we consider the reaction to be thermodynamically controlled. This is shown schematically in the right-hand side of Figure 1. Upon heating, the atomic mobility is high enough near T_c^K, but the transformation does

* To whom correspondence should be addressed. Tel: (617) 253-1581. Fax: (617) 258-6534. E-mail: gceder@mit.edu.

(1) Aydinol, M. K.; Kohan, A. F.; Ceder, G. *J. Power Sources* **1997**, *68*, 664−668.
(2) Van der Ven, A.; Aydinol, M. K.; Ceder, G. *J. Electrochem. Soc.* **1998**, *145*, 2149−2155.
(3) Van der Ven, A.; Ceder, G. *Electrochem. Solid-State Lett.* **2000**, *3*, 301−304.
(4) Morgan, D.; Van der Ven, A.; Ceder, G. *Electrochem. Solid-State Lett.* **2004**, *7*, A30−A32.
(5) Meng, Y. S.; Van der Ven, A.; Chan, M. K. Y.; Ceder, G. *Phys. Rev. B* **2005**, *72*, 172103.
(6) Maxisch, T.; Zhou, F.; Ceder, G. *Phys. Rev. B* **2006**, *73*, 104301.
(7) Wang, L.; Maxisch, T.; Ceder, G. *Phys. Rev. B* **2006**, *73*, 195107-1−195107-6.
(8) Zhou, F.; Cococcioni, M.; Marianetti, C. A.; Morgan, D.; Ceder, G. *Phys. Rev. B* **2004**, *70*, 235121.
(9) Anisimov, V. I.; Aryasetiawan, F.; Liechtenstein, A. I. *J. Phys.: Condens. Matter* **1997**, *9*, 767−808.
(10) Cococcioni, M.; De Gironcoli, S. *Phys. Rev. B* **2005**, *71*, 035105.

10.1021/cm0620943 CCC: $37.00
Published on Web 12/24/2006

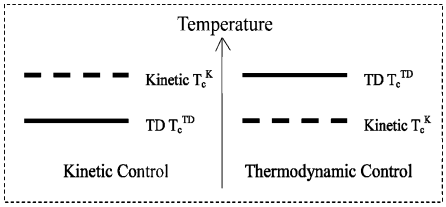

Figure 1. Schematic illustration of kinetically and thermodynamically controlled phase transitions. T_c^K and T_c^{TD} are the kinetic and thermodynamic critical transition temperatures, respectively.

not occur until T_c^{TD}, the thermodynamic transition temperature, is reached. For reactions with a low thermodynamic reaction temperature, the situation in the left-hand side of Figure 1 is more likely; in this case, the thermodynamic driving force for phase conversion already exists at low temperature, but the conversion occurs only when the ions achieve a high enough mobility. We refer to these as kinetically controlled transitions. Modeling the kinetics of phase transformations from first-principles is an unsolved problem in materials science. In the context of Li-electrode materials, useful qualitative information can be obtained by understanding how the mobility of a transition metal cation in a close-packed oxygen framework is determined by its energy difference in the octahedral and tetrahedral site, which is largely controlled by ligand field effects.[11,12] Ligand field theory predicts, for example, that Co^{3+} and Mn^{4+} are unlikely to be mobile because of their strong octahedral site preference, whereas Mn^{3+} and Mn^{2+} are expected to be mobile already at room temperature.[11] The transformation of a layered $Li_{0.5}MO_2$ compound to the spinel structure is an example of a kinetically controlled transformation. At partial state of delithiation, all layered Li_xMO_2 (with $x < 1$) compounds with the $R\bar{3}m$ structure (where M is a 3d transition metal) have a thermodynamic driving force for the conversion to spinel, even at 0 K, with a negative (exothermic) transformation enthalpy;[13] however, the temperature at which it occurs is determined by the mobility of the transition-metal cation and the amount of vacancies created by delithiation.[11,12] Ligand field energy differences between the octahedral and tetrahedral site explain very well, for example, why out of the three layered $Li_{0.5}MO_2$ (M = Mn, Co, Ni) compounds, $Li_{0.5}MnO_2$ is the least stable and $Li_{0.5}CoO_2$ the most stable.

Another class of transitions that is important for understanding the thermal stability of electrodes is those that reduce the average valence of the electrode by losing oxygen either through outgassing or oxidation of the electrolyte. Reactions that release O_2 gas have a large positive entropy of reaction and can always become favorable at a high enough temperature, even if they have positive reaction enthalpy. In this paper, we will mainly focus on these reduction reactions, though we will make occasional comments about the kinetic control of important reactions.

2. Methodology

All total energies in this work are calculated using the generalized gradient approximation (GGA) to density functional theory (DFT). Self-interactions and correlation effects due to localized d electrons have been addressed with the GGA+*U* method in its rotational invariant form.[14] The projected augmented wave (PAW)[15] method is used, as implemented in the Vienna Ab initio Simulation Package (VASP).[16] An energy cutoff of 500 eV and appropriate *k*-point meshes are chosen to ensure that the total energies are converged within 3 meV per formula unit.

Many of the decomposition reactions cause a change in the average oxidation states of the transition-metal ions and are accompanied by the release of O_2 gas. Our previous study has shown that in such cases, two substantial errors are present in GGA.[7] The first error originates from the overestimation of the binding energies of the O_2 molecule and the electron addition to oxygen when O^{2-} is formed. The magnitude of this error was estimated to be -1.36 eV per O_2 molecule.[7] To achieve reasonable and quantitative accuracy, we therefore increase all calculated oxidation energies by -1.36 eV. The second error in GGA is related to the correlation error in transition metals due to the localized 3d orbitals in GGA and can be alleviated through the use of the GGA+*U* method.[9] This approach treats the localized d orbitals with an explicit Hubbard term and cancels the self-interactions. The GGA+*U* treatment was shown to be crucial for obtaining accurate oxidation energies and Li-insertion voltages.[8] *U* parameters have been calculated self-consistently in some typical crystal structures for cathode materials.[8] On the basis of these results, we chose U values of 6, 5.5, and 4.2 eV for Ni in the Li−Ni−O_2 system, Co in the Li−Co−O_2 system, and Mn in the Li−Mn−O_2 system, respectively. The value of *U* tends to become smaller as the valence state of the ion decreases. Hence, these values of *U* may be somewhat too large for strongly reduced states (e.g., NiO and MnO).

Ternary Li−M−O_2 phase diagrams in this paper are constructed by projecting the vertices of the three-dimensional energy convex hull onto the two-dimensional Gibbs triangle, describing the Li−M−O_2 composition space. This construction assures that each point in the phase diagram represents the phase or combination of phases with the lowest energy. Introducing temperature into ab initio phase stability calculations is a complex procedure that involves the calculation of the relevant vibrational, configurational, and electronic excitations.[17−21] However, in reactions that involve the loss of oxygen, the reaction entropy is dominated by the creation of O_2 gas, and the effect of temperature is effectively to lower the chemical potential of O_2 in the system, thereby decreasing the free energy of reduced products. Hence, for the general decomposition reaction of a lithium transition metal oxide

$$Li_xM_yO_{z+z'} \rightarrow Li_xM_yO_z + z'/2\ O_2 \qquad (1)$$

the entropy change ΔS originates mainly from the oxygen gas released. Assuming the temperature dependence of the reaction

(11) Reed, J.; Ceder, G.; Van der Ven, A. *Electrochem. Solid-State Lett.* **2001**, *4*, A78−A81.
(12) Reed, J.; Ceder, G. *Chem. Rev.* **2004**, *104*, 4513.
(13) Van der Ven, A.; Ceder, G. *Phys. Rev. B* **1999**, *59*, 742−749.
(14) Dudarev, S. L.; Botton, G. A.; Savrasov, S. Y.; Humphreys, C. J.; Sutton, A. P. *Phys. Rev. B* **1998**, *57*, 1505−1509.
(15) Kresse, G.; Joubert, D. *Phys. Rev. B* **1998**, *59*, 1758−1775.
(16) Kresse, G.; Furthmüller, J. *Phys. Rev. B* **1996**, *54*, 11169−11186.
(17) Garbulsky, G. D.; Ceder, G. *Phys. Rev. B* **1994**, *49*, 6327−6330.
(18) Sanchez, J. M.; de Fontaine, D. *Phys. Rev. B* **1978**, *17*, 2926−2936.
(19) Asta, M.; McCormack, R.; de Fontaine, D. *Phys. Rev. B* **1993**, *48*, 748−766.
(20) Ceder, G. *Comput. Mater. Sci.* **1993**, *1*, 144−150.
(21) Ackland, G. J. *J. Phys.: Condens. Matter* **2002**, *14*, 2975−3000.

enthalpy is small compared to the $-T\Delta S$ term, we can approximate the reaction Gibbs free energy by

$$\Delta G = \Delta H - T\Delta S \approx -E^{\circ}(\mathrm{Li}_x\mathrm{M}_y\mathrm{O}_{z+z'}) + E^{\circ}(\mathrm{Li}_x\mathrm{M}_y\mathrm{O}_z) + z'/2E^{*}(\mathrm{O}_2) - T\Delta S \quad (2)$$

where E° refers to the total energy at 0 K and $E^{*}(\mathrm{O}_2)$ is the calculated energy of an O_2 molecule at 0 K plus 1.36 eV per O_2 molecule to compensate for the GGA error in O_2, as discussed in ref 7. This correction also includes the $P\Delta V$ contribution to the enthalpy.[7] Previous work has compared the calculated oxidation enthalpies at 0 K with the experimental values at room temperature for typical transition metal oxides and estimated the enthalpy difference to be less than 10 kJ per mole of O_2.[7] This is significantly smaller than the contribution from the entropy of O_2 gas formation, which is about 110 kJ/mol at 500 K.[22] Thus, in our approach, the temperature dependence in ΔG is exclusively given by the $-T\Delta S$ term, where ΔS corresponds to the oxygen gas entropy. A reference state with an oxygen partial pressure of 1 atm is assumed. The temperature for which the reaction Gibbs free energy in eq 2 equals zero is the thermodynamic transition temperature at which a stable compound on the left-hand side of reaction 1 becomes unstable with respect to compounds on the right-hand side of reaction 1.

$$T = \frac{\Delta H}{\Delta S} \approx \frac{-E^{\circ}(\mathrm{Li}_x\mathrm{M}_y\mathrm{O}_{z+z'}) + E^{\circ}(\mathrm{Li}_x\mathrm{M}_y\mathrm{O}_z) + z'/2E^{*}(\mathrm{O}_2)}{z'/2S(\mathrm{O}_2)} \quad (3)$$

The entropy for oxygen gas is a function of temperature and can be obtained from the *JANAF* thermochemistry tables.[22] We solve eq 3 iteratively: The entropy value for oxygen gas at room temperature is first used in eq 3 to estimate the thermodynamic transition temperature T. The entropy value for oxygen gas at the predicted temperature is then used to calculate the transition temperature T again. This iteration proceeds until the new predicted temperature T differs from the previous temperature value by less than 20 K.

3. Results

We test our approach on Li_xNiO_2, Li_xCoO_2, and $Li_xMn_2O_4$, three experimentally well-characterized systems, and show that their distinct behavior can be well-reproduced with our method.

3.1. Li_xNiO_2. Substantial delithiation of $LiNiO_2$ is known to lead to very unstable compounds that decompose at lower temperature than is the case for delithiated Li_xCoO_2 and $Li_xMn_2O_4$.[23] Thomas et al. suggested that $Li_{0.5}NiO_2$ undergoes a first-order transformation above 420 K to the cubic spinel phase $LiNi_2O_4$, which is stable up to 570 K.[24] Lee et al. have also investigated the composition and temperature dependence of the thermal behavior of Li_xNiO_2:[25] They find that for $x > 0.5$, Li_xNiO_2 decomposes into layered $LiNiO_2$ and spinel $LiNi_2O_4$, whereas for $x < 0.5$, Li_xNiO_2 converts to spinel accompanied by the release of oxygen. A further temperature increase leads to the formation of a rocksalt phase in which Li and Ni ions are disordered, with oxygen release at all compositions. Figure 2 illustrates the possible reaction scheme and the corresponding structure changes during the transformation from the layered to the rocksalt structure. Guilmard and co-workers have reported that the transformation from layered-to-spinel involves the migration of Ni cations from the Ni layer into the Li layer, and a displacement of Li from the octahedral to the tetrahedral sites.[26] Such spinel phases obtained through cation migrations are not perfectly ordered and intermediate pseudospinel structures always appear.[26] Additionally, it has been reported that further decomposition into the rocksalt structure is an exothermic reaction that involves the random redistribution of Li and Ni cations across the cation layers and the evolution of oxygen.[27] Lee et al. observed that for $x \geq 0.5$, the reaction heat when the layered structure transforms to spinel decreases linearly with increasing x in Li_xNiO_2. However, for $x < 0.5$ the reaction heat increases as x approaches 0.5.[25] They argued that the change in heat flow near $x = 0.5$ is due to the oxygen release when $x < 0.5$ and interpreted the thermal behavior of Li_xNiO_2 as an overlap of the exothermic reaction to form a spinel and the endothermic oxygen evolution reaction.

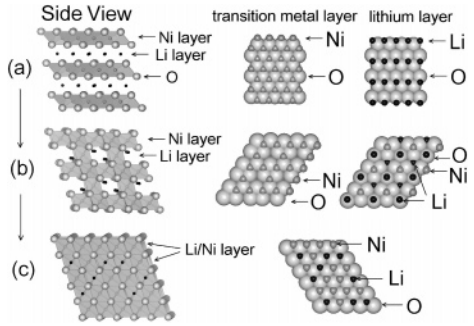

Figure 2. Possible reaction scheme and structure changes during the transition of (a) layered structure (R-3m) Li_xNiO_2 to (b) spinel structure ($Fd3m$) $LiNi_2O_4$ and further to (c) disordered rocksalt structure ($Fm3m$) with a composition of $Li_{0.33}Ni_{0.67}O$. In (c), the metal layers are identical in composition.

To clarify the origin of heat generation during the phase transformations, particularly for the decomposition reaction of a spinel phase into a rocksalt phase, we have calculated the ternary phase diagram (see Figure 3) for Li−Ni−O_2 at 0 K using GGA+U with U on Ni = 6 eV, which is the self-consistently calculated value for Ni^{4+} ions in the layered structure.[8] Note that this is an approximation, because the U value depends on the oxidation state and crystal environment, both of which are changing during the decomposition. However, the U value needs to be fixed to one consistent value in order to have reasonable reaction energies. The diagram shows the stable compounds and three-phase equilibria at 0 K. Delithiation of layered $LiNiO_2$ proceeds along the line that connects this composition with NiO_2. There are no thermodynamically stable partially delithiated states (compositions 4, 5, and 6 in Figure 3 were tested), even though metastable Li-vacancy ordered states are known to exist.[28−30] The delithiation path for $0.5 < x < 1$ lies on

(22) Chase, M. W. *NIST-JANAF Thermochemical Tables*, 4th ed.; American Institute of Physics: Melville, NY, 1998.
(23) Dahn, J. R.; Fuller, E. W.; Obrovac, M.; Sacken, U. v. *Solid State Ionics* **1994**, *69*, 265−270.
(24) Thomas, M. G. S. R.; David, W. I. F.; Goodenough, J. B.; Groves, P. *Mater. Res. Bull.* **1985**, *20*, 1137−1146.
(25) Lee, K. K.; Yoon, W. S.; Kim, K. B.; Lee, K. Y.; Hong, S. T. *J. Power Sources* **2001**, *97−98*, 321−325.
(26) Guilmard, M.; Croguennec, L.; Denux, D.; Delmas, C. *Chem. Mater.* **2003**, *15*, 4476−4483.
(27) Arai, H.; Okada, S.; Sakurai, Y.; Yamaki, J. *Solid State Ionics* **1998**, *109*, 295−302.
(28) de Dompablo, M. E. A. Y.; Van der Ven, A.; Ceder, G. *Phys. Rev. B* **2002**, *66*, 064112.

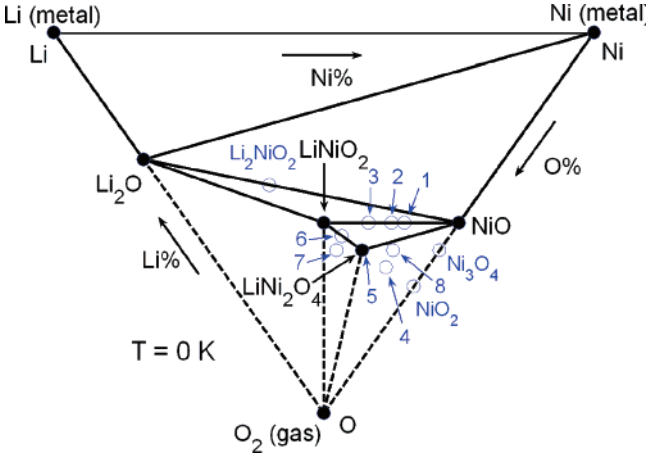

Figure 3. Calculated ternary phase diagram for Li−Ni−O_2 at 0 K. Dashed lines indicate that the triangles connecting O_2 depend on pressure. Filled (unfilled) circles indicate stable (unstable) compounds. Points labeled as 1−3 represent rocksalt structures of composition $Li_xNi_{1-x}O$ with $x = 0.2$, 0.25, and 0.33, respectively. Points labeled as 4−6 are layered structures of composition Li_xNiO_2 with $x = 0.25$, 0.5, and 0.75, respectively. Points labeled as 7 and 8 are pseudospinel structures of composition $(Li_3)_{tet}(LiNi_5^{4+})_{oct}O_{12}$ and $(Li_3Ni_2^{2+})_{tet}(Ni_7^{3+}\ Ni_3^{4+})_{oct}O_{20}$. Li_2NiO_2 has an orthorhombic structure.[68] Ni_3O_4 has a spinel structure $(Ni^{2+})_{tet}(Ni_2^{3+})_{oct}O_4$.

the edge of the $LiNiO_2$−$LiNi_2O_4$−NiO equilibrium triangle so that the delithiated phases are unstable with respect to the formation of spinel

$$Li_xNiO_2(\text{layered}) \rightarrow (1-x)LiNi_2O_4(\text{spinel}) + (2x-1)LiNiO_2(\text{layered}) \quad (4)$$

This reaction occurs without a loss of oxygen. For $x < 0.5$, the situation is qualitatively different, as the delithiation path cuts through the $LiNi_2O_4$−NiO−O_2 equilibrium triangle; this indicates that the layered phase may degrade through the formation of O_2 gas, spinel $LiNi_2O_4$, and NiO

$$Li_xNiO_2(\text{layered}) \rightarrow xLiNi_2O_4(\text{spinel}) + (1-2x)NiO(\text{rocksalt}) + \frac{(1-2x)}{2}O_2 \quad (5)$$

We also computed the energy of a pseudospinel $(Li_3Ni_2^{2+})_{tet}(Ni_7^{3+}Ni_3^{4+})_{oct}O_{20}$, as has been suggested to occur experimentally,[26] but did not find it to be stable. It may become more stable at higher temperature because of the mixing entropy induced by Li and Ni sharing sites. An alternative explanation is that the pseudospinel is observed in experiments as a transient state toward the formation of $LiNi_2O_4$ spinel and NiO.

The calculated enthalpies for reactions 4 and 5 are shown in Figure 4. In agreement with experiments, we find that the conversion from the layered structure to spinel is exothermic. The measured value at $x = 0.75$ is more negative than our calculated number, though we point out that the excess Ni, which is always present in experimental samples, may change the reaction energy. At $x = 0.25$, we find that the conversion of the layered structure to a perfectly ordered

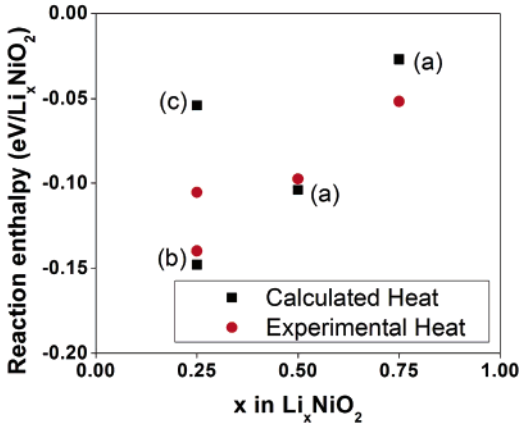

Figure 4. Calculated and experimental enthalpies for the reaction of layered Li_xNiO_2 to spinel. Circles are experimental results.[25,31] Squares are calculated results. Points labeled as (a) are calculated according to reaction 4. Point labeled as (b) is calculated according to reaction 5. Point labeled as (c) indicates the formation of pseudospinel phase $(Li_3Ni_2^{2+})_{tet}(Ni_7^{3+}\ Ni_3^{4+})_{oct}\ O_{20}$ plus oxygen gas in the layered-to-spinel conversion.

spinel with NiO and O_2 gas gives an even more negative reaction heat, whereas the formation of the pseudospinel phase generates much less heat. This is in accordance with the spinel being the most stable reaction product. The two available experimental values at $x = 0.25$[25,31] fall between our calculated reaction heat for forming spinel and pseudospinel, which may indicate that either an intermediate phase between the two structures (more ordered pseudospinel) or a mixture of the two phases is formed. The phase diagram in Figure 3 and the heats of reaction in Figure 4 agree well with experiments, indicating that our approach can at least predict the thermodynamically stable phases.

Figure 3 shows that partially delithiated layered phases are thermodynamically unstable against spinel. Whether these transitions occur will depend on the mobility of the Ni ions. Layered to spinel conversion requires the migration of Ni ions into the Li slab space, passing through the intermediate tetrahedral sites. Ni^{4+} is known to have a strong octahedral site preference due to its filled t_{2g} states,[12] whereas Ni^{3+} has a somewhat weaker octahedral preference. Both ions are therefore not very mobile, which explains the kinetic stability of the material at room temperature and slightly above.[24] Given that the transformation from the layered structure to spinel requires elevated temperature, it is possible that the $LiNi_2O_4$ spinel becomes thermodynamically unstable before it can be achieved kinetically from the layered phase. Figure 5 shows the calculated temperature evolution of the system. The temperatures in the figure are estimated using eq 3. As temperature increases, we find that spinel $LiNi_2O_4$ becomes thermodynamically unstable toward products with a lower average oxidation state of Ni according to the following reaction

$$LiNi_2O_4(\text{spinel}) \rightarrow LiNiO_2(\text{layered}) + NiO(\text{rocksalt}) + (1/2)O_2 \quad (6)$$

In this reaction, half of the Ni cations are reduced to Ni^{2+}.

(29) Delmas, C.; Menetrier, M.; Croguennec, L.; Levasseur, S.; Peres, J. P.; Pouillerie, C.; Prado, G.; Fournes, L.; Weill, F. *Int. J. Inorg. Mater.* **1999**, *1*, 11−19.
(30) Peres, J. P.; Weill, F.; Delmas, C. *Solid State Ionics* **1999**, *116*, 19−27.
(31) Zhang, Z.; Fouchard, D.; Rea, J. R. *J. Power Sources* **1998**, *70*, 16−20.

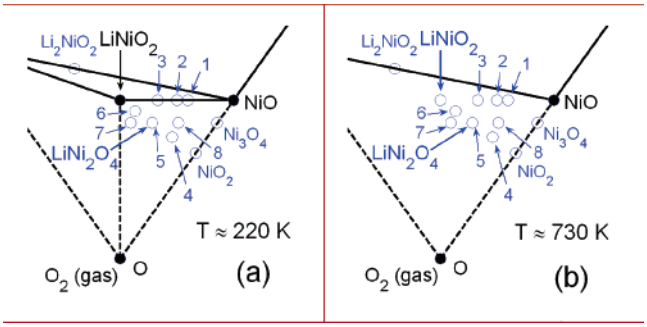

Figure 5. Temperature evolution of ternary phase diagram of Li−Ni−O_2. Filled (unfilled) circles indicate stable (unstable) compounds. Points labeled as 1−8 are the same as those in Figure 4.

The reaction enthalpy of reaction 6 is calculated to be 218 meV (endothermic) per formula unit of $LiNi_2O_4$. The value of this decomposition heat can be more positive if a disordered rocksalt structure is formed instead of the mixture of $LiNiO_2$ and NiO. The temperature at which spinel becomes thermodynamically unstable is quite low in our calculations. Several factors may influence this result. Inaccuracies in DFT, the chosen U values, or the entropy approximations in eq 2 and 3 could all modify this temperature. In addition, real $LiNiO_2$ always contains Ni excess and the created Ni^{2+} may stabilize the material somewhat against reduction.

Hence, if spinel is unstable at room temperature or its formation is kinetically limited, direct conversion to $LiNiO_2$, NiO, and O_2 will occur according to

$$\mathrm{Li}_x\mathrm{NiO}_2(\text{layered}) \rightarrow x\mathrm{LiNiO}_2(\text{layered}) + (1-x)\mathrm{NiO}(\text{rocksalt}) + \frac{(1-x)}{2}\mathrm{O}_2 \quad (7)$$

The reaction enthalpy of reaction 7 is calculated to be 28, 5, and −93 meV per formula unit of Li_xNiO_2, respectively, for $x = 0.75$, 0. 5, and 0.25, indicating that the heat generation depends on Li content x. The reaction enthalpy in reaction 7 changes from positive to negative as the amount of oxygen generated increases. Arai et al.[32] have reported that the overall layered to rocksalt transformation is endothermic for $x \geq 0.4$ and exothermic for $x < 0.3$, which is consistent with our calculations.

3.2. Li_xCoO_2. Partially delithiated $LiCoO_2$ in the layered ($R\bar{3}m$) structure is known to be metastable, and the material loses oxygen at temperatures above 470 K.[23,33,34] Dahn et al. suggested that delithiated materials decompose to stoichiometric $LiCoO_2$ and spinel Co_3O_4 according to the following reactions[23]

$$\mathrm{Li}_x\mathrm{CoO}_2(\text{layered}) \rightarrow x\mathrm{LiCoO}_2(\text{layered}) + \frac{(1-x)}{3}\mathrm{Co}_3\mathrm{O}_4(\text{spinel}) + \frac{(1-x)}{3}\mathrm{O}_2 \quad (8)$$

Differential scanning calorimetry (DSC) measurements of the chemically dilithiated Li_xCoO_2 without the presence of electrolyte indicates that reaction 8 is an exothermic reaction and that the material is less reactive as x increases.[33,34]

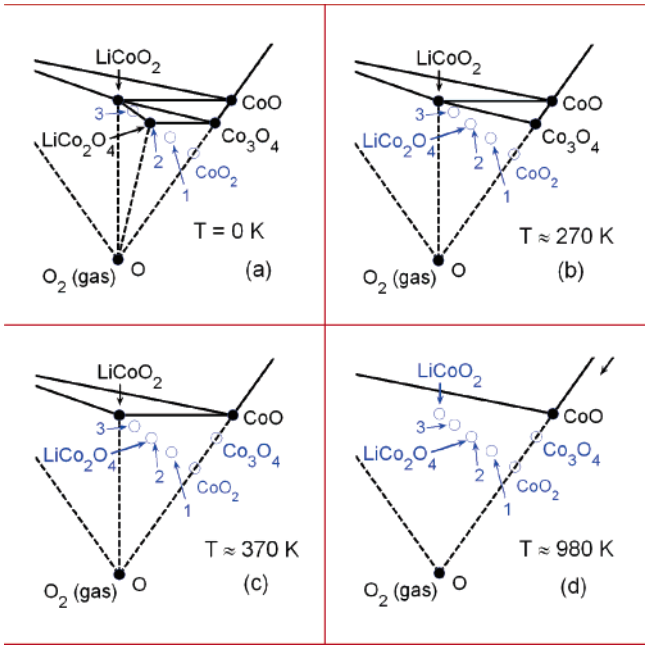

Figure 6. Ternary phase diagram of Li−Co−O_2 at 0 K and its temperature evolution. Filled (unfilled) circles indicate stable (unstable) compounds. Points labeled as 1−3 are layered structures of composition Li_xCoO_2 with $x = 0.25$, 0.5, and 0.75, respectively.

Figure 6 shows the calculated ternary diagram for Li−Co−O_2 at $T = 0$ K and the temperature evolution of the system. Similar to the situation in the Ni system, our $T = 0$ K calculation (see Figure 6a) confirms that partially delithiated Li_xCoO_2 (compositions 1, 2, and 3 in Figure 6 were tested) is thermodynamically unstable against the formation of spinel $LiCo_2O_4$ and some other products.[12,13,35] Spinel Co_3O_4 appears as a stable phase in the Li−Co−O_2 phase diagram. This is different from the Ni system, because Ni_3O_4 is not stable and NiO forms instead. For $0.5 < x < 1$, the delithiation path lies on the edge of the $LiCoO_2$−$LiCo_2O_4$−Co_3O_4 equilibrium triangle so that delithiated phases form spinel through the reaction

$$\mathrm{Li}_x\mathrm{CoO}_2(\text{layered}) \rightarrow (1-x)\mathrm{LiCo}_2\mathrm{O}_4(\text{spinel}) + (2x-1)\mathrm{LiCoO}_2(\text{layered}) \quad (9)$$

For $x < 0.5$, the delithiation path cuts through the $LiCo_2O_4$−Co_3O_4−O_2 equilibrium triangle, indicating that the layered phase may degrade with a loss of O_2

$$\mathrm{Li}_x\mathrm{CoO}_2(\text{layered}) \rightarrow x\mathrm{LiCo}_2\mathrm{O}_4(\text{spinel}) + \frac{(1-2x)}{3}\mathrm{Co}_3\mathrm{O}_4(\text{spinel}) + \frac{(1-2x)}{3}\mathrm{O}_2 \quad (10)$$

The loss of oxygen here is less than the amount in the Ni system (on a per formula unit basis) because of the reduction to Co_3O_4 in the Co system, as compared to NiO in the Ni materials.

The calculated reaction enthalpies indicate that reactions 9 and 10 are both exothermic at the four compositions we

(32) Arai, H.; Sokurai, Y. *J. Power Sources* **1999**, *81*, 401−405.
(33) Yamaki, J.; Baba, Y.; Katayama, N.; Takatsuji, H.; Egashira, M.; Okada, S. *J. Power Sources* **2003**, *119*, 789−793.
(34) Baba, Y.; Okada, S.; Yamaki, J. *Solid State Ionics* **2002**, *148*, 311−316.
(35) Wolverton, C.; Zunger, A. *J. Electrochem. Soc.* **1998**, *145*, 2424−2431.

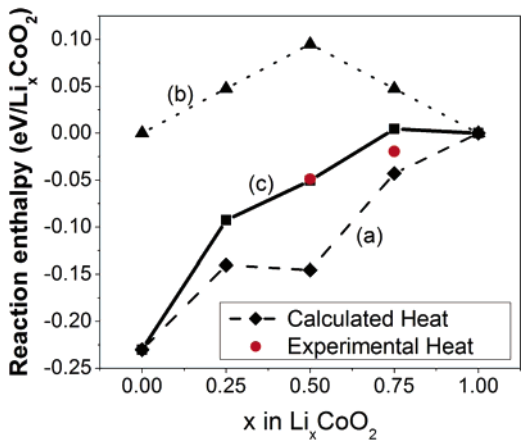

Figure 7. Calculated and experimental enthalpies for the decomposition of layered Li_xCoO_2 as a function of the Li composition x: (a) diamond points are the calculated reaction heat for the layered-to-spinel composition (reactions 9 and 10 in the text); (b) triangle points represent the reaction heat for the spinel decomposition (reaction 11 in the text); (c) square points show the overall reaction heat for the direct decomposition of layered Li_xCoO_2 (reaction 8 in the text). The two available experimental values[33] are marked by circles.

tested (see line a in Figure 7). Thus, the conversion from the partially delithiated layered to the spinel structure is energetically favored at all temperatures and will occur at a temperature at which the Co cation gains enough mobility. In our calculations, spinel $LiCo_2O_4$ becomes thermodynamically unstable as temperature increases (see Figure 6b−d) and decomposes into layered $LiCoO_2$, Co_3O_4, and O_2

$$LiCo_2O_4(\text{spinel}) \rightarrow LiCoO_2(\text{layered}) + (1/3)Co_3O_4(\text{spinel}) + (1/3)O_2 \quad (11)$$

Reaction 11 is calculated to be endothermic, with an enthalpy change of 190 meV per formula unit of $LiCo_2O_4$. Hence, the equilibrium reaction path for delithiated layered Li_xCoO_2 would be the exothermic conversion of partially delithiated layered Li_xCoO_2 to spinel followed by the endothermic decomposition of spinel $LiCo_2O_4$ to layered $LiCoO_2$ and Co_3O_4.

Whether in reality the spinel appears as a stable intermediate or direct decomposition of the layered phase occurs depends on whether the temperature at which the Co ions become mobile is above or below the thermodynamic transition temperature for the spinel decomposition reaction. The kinetic limitation of converting the partially delithiated layered Li_xCoO_2 to spinel was suggested by previous theoretical work to be due to the high activation barrier found for Co migration.[11,12] Ligand field splitting of electron levels gives Co^{3+} a very strong preference for octahedral sites, limiting its ability to hop through tetrahedral sites. Slow reaction kinetics for the decomposition reaction 8 is also observed in experimental studies,[31,34] particularly for the highly discharged states. If spinel $LiCo_2O_4$ does not form, decomposition would proceed according to reaction 8, as suggested by Dahn.[23]

In Figure 7, we show the calculated reaction heat for the direct decomposition of layered Li_xCoO_2 following reaction 8. The dashed line shows the contribution from the exothermic layered-to-spinel conversion according to reactions 9 and 10, and the dotted line shows the contribution from the endothermic spinel decomposition according to reaction 11. The overall reaction heat of reaction 8 is the combination of the two reaction heats and is calculated to be −93, −51, and 5 meV per formula unit of Li_xCoO_2, respectively, for $x = 0.25$, 0.5, and 0.75. The reaction heat changes from negative to positive as x increases, similar to what we find in the Ni system. The result for the reaction heat at $x = 0.5$ compares well with Yamaki et.al's DSC measurements of −50 J/g (−49 meV per formula unit of Li_xCoO_2).[33] Their measurement at $x = 0.75$ gives an exothermic reaction enthalpy of −20 J/g (−20 meV per formula unit of Li_xCoO_2), which is between the heat released in the layered-to-spinel conversion and the heat resulting from spinel decomposition. This may imply that in experiments reaction 8 in $Li_{0.75}CoO_2$ is not complete.

3.3. $Li_xMn_2O_4$. Lithium manganese oxides that have been studied as possible positive electrode materials are $LiMnO_2$ with the monoclinically distorted α-$NaFeO_2$-type layered structure (*C*2/*m*),[36−40] $LiMnO_2$ with the orthorhombic structure (*Pmnm*),[41,42] and spinel (*Fd*-3*m* or $I4_1/amd$) $LiMn_2O_4$.[41−43] Mishra et al. studied the relative stability of Li_xMnO_2 in different crystal structures at $x = 0$, 0.5, and 1.[44,45] At the composition MnO_2, the layered structure is more stable compared to the spinel (λ-MnO_2) and orthorhombic forms. These are all structures with ABC oxygen stacking. Pyrolusite (β-MnO_2) with AB oxygen stacking is generally regarded as the most stable structure at this composition.[46] In agreement with experiments and with previous theoretical work,[44,47,48] we find the orthorhombic $LiMnO_2$ structure with antiferromagnetic spin arrangement to be lower in energy than the fully lithiated spinel $Li_2Mn_2O_4$ or layered structure. The layered and orthorhombic structures are known to undergo rapid transformations to the spinel structure upon delithiation.[40,49−51] Our calculated phase diagram confirms the stability of spinel $LiMn_2O_4$ along the delithiation path of orthorhombic or layered $LiMnO_2$. The rapid nature of this transformation was previously attributed to the ease by which Mn^{3+} disproportionates and moves through the tetrahedral sites.[12] Spinel $Li_xMn_2O_4$ is not observed to be susceptible to any major structural transformation upon electrochemical

(36) Armstrong, A. R.; Bruce, P. G. *Nature* **1996**, *381*, 499−500.
(37) Capitaine, F.; Gravereau, P.; Delmas, C. *Solid State Ionics* **1996**, *89*, 197−202.
(38) Armstrong, A. R.; Robertson, A. D.; Bruce, P. G. *Electrochim. Acta* **1999**, *15*, 285−294.
(39) Bruce, P. G.; Armstrong, A. R.; Gitzendanner, R. L. *J. Mater. Chem.* **1999**, *9*, 193−198.
(40) Shao-Horn, Y.; Hackney, S. A.; Armstrong, A. R.; Bruce, P. G.; Gitzendanner, R.; Johnson, C. S.; Thackeray, M. M. *J. Electrochem. Soc.* **1999**, *146*, 2404−2412.
(41) Thackeray, M. M. *Prog. Solid State Chem.* **1997**, *25*, 1−71.
(42) Winter, M.; Besenhard, J. O.; Spahr, M. E.; Novak, P. *Adv. Mater.* **1998**, *10*, 725−763.
(43) Bruce, P. G. *Chem. Commun.* **1997**, *19*, 1817−1824.
(44) Mishra, S. K.; Ceder, G. *Phys. Rev. B* **1999**, *59*, 6120−6130.
(45) Ceder, G.; Mishra, S. K. *Electrochem. Solid-State Lett.* **1999**, *2*, 11.
(46) Chabre, Y.; Pannetier, J. *Prog. Solid State Chem.* **1995**, *23*, 1−130.
(47) Dittrich, G.; Hoppe, R. *Z. Anorg. Allg. Chem.* **1969**, *368*, 262−270.
(48) Hoppe, R.; Brachtel, G.; Jansen, M. *Z. Anorg. Allg. Chem.* **1975**, *417*, 1−10.
(49) Blyr, A.; Sigala, C.; Amatucci, G.; Guyomard, D.; Chabre, Y.; Tarascon, J. M. *J. Electrochem. Soc.* **1998**, *145*, 194−209.
(50) Chiang, Y. M.; Sadoway, D. R.; Jiang, Y.; Huang, B.; Wang, H. *Electrochem. Solid-State Lett.* **1999**, *2*, 107−110.
(51) Vitins, G.; West, K. *J. Electrochem. Soc.* **1997**, *144*, 2587−2592.

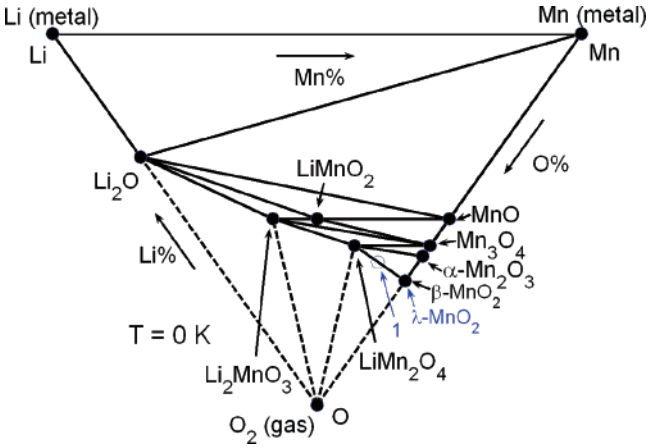

Figure 8. Calculated ternary phase diagram for Li−Mn−O_2 at 0 K. Point labeled as 1 is the half delithiated spinel with a composition of $Li_{0.5}Mn_2O_4$. Filled (unfilled) circles indicate stable (unstable) compounds.

cycling over the range $0 \le x \le 2$, though the practical cycling of Li is limited to $0 \le x \le 1$ because of the asymmetric lattice expansion of $Li_{1+x}Mn_2O_4$ induced by the Jahn−Teller effect.[41] Our phase diagram in Figure 8 shows that delithiated spinel (composition 1 was tested in Figure 8) is metastable with respect to β-MnO_2 formation. As this transformation requires reshuffling of the oxygen layers, it is unlikely to occur at low temperature. Thus, in contrast to Li_xNiO_2 and Li_xCoO_2, $LiMn_2O_4$ is not thermodynamically unstable with respect to oxygen loss upon delithiation, because the β-MnO_2−$LiMn_2O_4$ tie line is part of a stable three-phase triangle in the phase diagram. Hence, we will focus on the spinel $Li_xMn_2O_4$ at composition $x = 0$ and 1 and discuss the possible degradation mechanism for the material at elevated temperatures. Schilling et al. reported that the fully delithiated $Li_xMn_2O_4$ ($x = 0$) undergoes an exothermic transition to β-MnO_2 at 540 K followed by an endothermic decomposition into α-Mn_2O_3 at 820 K.[52] For the cubic spinel $LiMn_2O_4$, experimental studies have reported various phase transitions accompanied by the loss of oxygen at high temperature:[52−56] Tsuji et al. reported that the material has weight loss in air around 960 K, with two more weight loss peaks at 1210 and 1350 K. Monoclinic Li_2MnO_3 appears as the first decomposition product, followed by orthorhombic $LiMnO_2$ and tetragonal spinel Mn_3O_4.[53]

According to our calculated Li−Mn−O_2 ternary phase diagram (see Figure 8), cubic spinel $LiMn_2O_4$ appears in the diagram as a stable phase. As the temperature increases, $LiMn_2O_4$ decomposes in several characteristic stages. In going from Figure 9b to Figure 9c, $LiMn_2O_4$ has decomposed into monoclinic Li_2MnO_3 and tetragonal spinel Mn_3O_4. Further increasing the temperature toward Figure 9d leads to a reaction in which Li_2MnO_3 disappears by reacting with some of the Mn_3O_4 to form orthorhombic $LiMnO_2$. Further

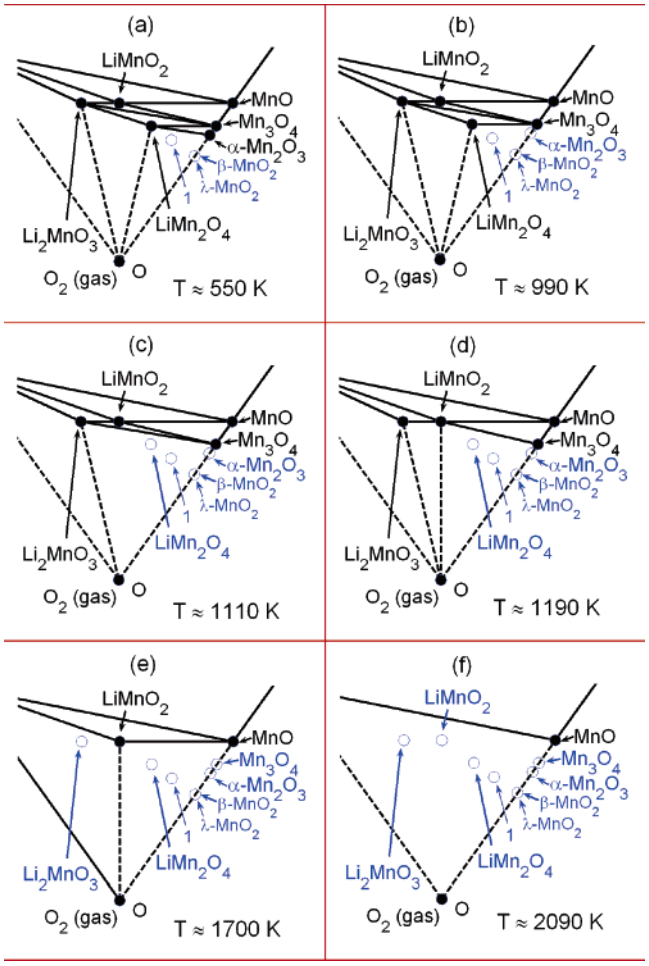

Figure 9. Temperature evolution of ternary phase diagram of Li−Mn−O_2. Filled (unfilled) circles indicate stable (unstable) compounds. Point labeled as 1 is the half delithiated spinel with a composition of $Li_{0.5}Mn_2O_4$.

reactions (panels e and f of Figure 9) lead to the formation of MnO and disappearance of all ternary compounds from the phase diagrams. The phases appearing as decomposition products of $LiMn_2O_4$ compare well with those observed in Tsuji's experimental thermal stability studies at this Li content.[53] The calculated ternary phase diagram also provides the decomposition information for the fully delithiated $LiMn_2O_4$ (λ-Mn_2O_4 in Figures 8 and 9): λ-Mn_2O_4 is unstable compared to β-MnO_2 and is gradually reduced to α-Mn_2O_3, Mn_3O_4, and MnO according to our phase diagram (Figures 8 and 9a,b,e). Decomposition products β-MnO_2, α-Mn_2O_3, and Mn_3O_4 are observed in experiments,[52] but the highly reduced product MnO has not been reported.

Because Li_2MnO_3 is only stable as a decomposition product in a narrow temperature range, we consider directly the decomposition of spinel $LiMn_2O_4$ into orthorhombic $LiMnO_2$, Mn_3O_4, and O_2 following the reactions below

$$LiMn_2O_4 \rightarrow LiMnO_2 + (1/3)Mn_3O_4 + (1/3)O_2 \quad (12)$$

The reaction enthalpy of reaction 12 is calculated to be 0.984 eV per formula unit of $LiMn_2O_4$. This is close to Tsuji's experimental results of 547 ± 70 J/g (1.035 eV per formula unit of $LiMn_2O_4$).[53] Note that reaction 12 is calculated to be highly endothermic compared to the decomposition of spinel $LiNi_2O_4$ and $LiCo_2O_4$, indicating a thermodynamically

(52) Schilling, O.; Dahn, J. R. *J. Electrochem. Soc.* **1998**, *145*, 569−575.
(53) Tsuji, T.; Umakoshi, H.; Yamamura, Y. *J. Phys. Chem. Solids* **2005**, *66*, 283−287.
(54) Massarotti, V.; Capsoni, D.; Bini, M. *Solid State Commun.* **2002**, *122*, 317−322.
(55) Thackeray, M. M.; Mansuetto, M. F.; Bates, J. B. *J. Power Sources* **1997**, *68*, 153−158.
(56) Tarascon, J. M.; Coowar, F.; Amatuci, G.; Shokoohi, F. K.; Guyomard, D. G. *J. Power Sources* **1995**, *54*, 103−108.

controlled decomposition of $LiMn_2O_4$. However, the large and positive reaction entropy from oxygen gas can make the decomposition reaction 12 favorable at high temperature.

3.4. Oxidation of Electrolytes. In practical batteries, it is the stability of the cathode materials in the organic electrolyte that is important. To better simulate the safety of real battery systems, we need to include the effects of the electrolyte in our model. Previous experimental studies of the reactions between electrolyte and cathode materials have shown that cathode materials can be more reactive in the presence of electrolyte and that the reaction heat is consistent with what is expected from the combustion of electrolyte by the oxygen gas released as the cathode material decomposes.[33,34,57,58] The electrolyte can modify the stability of pure cathode results in three ways:

(1) It can catalyze electrode decomposition reaction at the electrode surface.

(2) Its combustion equilibrium creates a low oxygen chemical potential in the system, which will reduce the electrode at lower temperature than for a pure cathode.

(3) Its combustion with oxygen from the electrode decomposition adds exothermic heat to the overall reaction.

We will focus on the thermodynamics of the reactions between electrolyte and cathode materials and the modifications to the heat flow. As a case study, ethylene carbonate (EC) is selected to represent the electrolyte in our study. In reality, EC is always used together with diethyl carbonate (DEC), and both of them can combust.

The combustion of electrolyte depends upon the environmental oxygen chemical potential. If we consider the full combustion of EC, the reaction can be expressed by

$$2C_3H_4O_3 + 5O_2 \rightarrow 6CO_2 + 4H_2O \qquad (13)$$

We calculated the energy of EC in its solid state with a space group of $C2/c$[59] and added the experimental measured heat of melting[60] to obtain the energy of its liquid state. The other species were calculated as molecules. The resulting reaction heat of −10.577 eV per formula of EC is in reasonable agreement with the experimental value of −11.187 eV per formula of EC.[61] The critical oxygen chemical potential that turns the reaction Gibbs free energy of reaction 13 negative is given by

$$\mu_{O_2} = 6/5\mu_{CO_2} + 4/5\mu_{H_2O} - 2/5\mu_{C_3H_4O_3} \approx 6/5(E^\circ_{CO_2} - TS_{CO_2}) + 4/5(E^\circ_{H_2O} - TS_{H_2O}) - 2/5(E^\circ_{C_3H_4O_3} - TS_{C_3H_4O_3}) \qquad (14)$$

Here, E° represents the energy of each species at 0 K in a pure molecule or solid state and S implies the entropy at temperature T. For the combustion of EC to be thermodynamically favorable, oxygen has to be provided by the environment at a chemical potential larger than the value given in eq 14. Figure 10 shows this critical oxygen chemical potential in eq 14 as a function of temperature. The oxygen chemical potential of oxygen gas (at a pressure of 1 atm) is also plotted in Figure 10 and lies much higher than the critical oxygen chemical potential for the combustion reaction 13. The third relevant oxygen chemical potential is the one established by an O_2-producing decomposition reaction. In that case

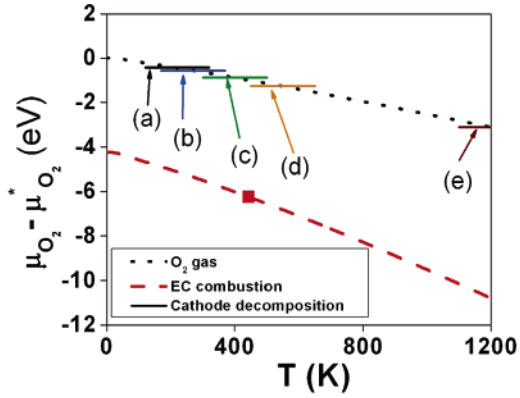

Figure 10. Calculated critical oxygen chemical potentials μ_{O_2} as a function of temperature. All μ_{O_2} values are shown with their differences from the oxygen chemical potential at 0 K (denoted as $\mu^*_{O_2}$). Dotted line shows the change in μ_{O_2} for oxygen gas as temperature increases. Dashed line shows the critical μ_{O_2} for the combustion reaction of ethylene carbonate (EC). Solid lines show the critical μ_{O_2} for different decomposition reactions of cathode materials. See the text for details about the specifications of each solid line. The flash point of EC is marked with a square.

$$\mu_{O_2} = \frac{2}{z'}(\mu_{Li_xM_yO_{z+z'}} - \mu_{Li_xM_yO_z}) \approx \frac{2}{z'}(E^\circ(Li_xM_yO_{z+z'}) - E^\circ(Li_xM_yO_z)) \qquad (15)$$

This equilibrium oxygen chemical potential is independent of temperature if the reaction energies on the right-hand side of eq 15 are temperature independent. In Figure 10, we also plotted this chemical potential for several decomposition reactions of the three cathode materials evaluated in this paper. Solid lines a and b in Figure 10 give the decomposition reactions of spinel $LiNi_2O_4$ and $LiCo_2O_4$ according to reactions 6 and 11, respectively; line c represents the decomposition of Co_3O_4 into CoO; line d represents the decomposition of λ-Mn_2O_4 into α-Mn_2O_3; line e indicates the decomposition of spinel $LiMn_2O_4$ following reaction 12. Note that lower oxygen chemical potentials in these decomposition reactions indicate higher stability, i.e., the system has less power to oxidize its environment or release oxygen. At a temperature at which the critical oxygen chemical potential for the decomposition of cathode material equals the chemical potential of oxygen gas, the decomposition reaction becomes thermodynamically favorable and oxygen gas is spontaneously generated from the cathode materials. It can also be seen from Figure 10 that the critical oxygen potentials for cathode decomposition are all above the one for the combustion reaction of the electrolyte, indicating that the reduction of cathode materials by the electrolyte is thermodynamically possible and can occur at the surface of cathodes. However, at low-temperature, it is unlikely that this occurs in bulk for the same reason that EC does not

(57) MacNeil, D. D.; Dahn, J. R. *J. Electrochem. Soc.* **2001**, *148*, A1205−A1210.
(58) MacNeil, D. D.; Dahn, J. R. *J. Electrochem. Soc.* **2001**, *148*, A1211−A1215.
(59) Brown, C. J. *Acta Crystallogr.* **1954**, *7*, 92−96.
(60) *60. Infotherm Thermophysical Properties Database*; FIZ CHEMIE: Berlin, 2005.
(61) Lide, D. R. *CRC Handbook of Chemistry and Physics*; CRC Press: Cleveland, OH, 1977.

spontaneously combust in air even though its thermodynamics allow it to. A more likely scenario is that electrolyte combustion by a charged cathode can only start at a temperature above its flash point and high enough to favor oxygen release from the cathode.

Under such a scenario, the temperature at which the bare electrode (i.e., without electrolyte) releases O_2 gas is still the critical temperature at which decomposition starts, but the presence of the electrolyte significantly modifies the reaction heat and enhances decomposition by further heating the system. Hence, although this is not a true catalytic effect, the heat generation by the electrolyte may help sustain the cathode decomposition reaction at a lower temperature than when no electrolyte is present.

Our results confirm the known hierarchy of safety issues in cathode materials. Even though it suffers from other capacity loss problems, spinel $LiMn_2O_4$ is a stable and safe material. Even the fully delithiated spinel Mn_2O_4 requires a high temperature to initialize decomposition with oxygen loss (line d in Figure 10). In the presence of electrolyte, the layered $LiNiO_2$ and $LiCoO_2$ have more safety issues, because the delithiated phases at low Li concentration can decompose with a loss of oxygen. The electrolyte plays the role of oxygen sink and creates a highly exothermic reaction, which further facilitates the decomposition of layered Li_xMO_2. Taking $Li_{0.5}CoO_2$ as an example, lines b and c of Figure 10 show that around the flash point of EC, $Li_{0.5}CoO_2$ can decompose into Co_3O_4 or CoO with the release of oxygen. This is consistent with what is found by MacNeil et al. in their experimental study.[57] If EC is considered to be in excess and a full combustion is assumed, the possible reactions between EC and $Li_{0.5}CoO_2$ can be summarized as

$$Li_{0.5}CoO_2 + (1/15)C_3H_4O_3 \rightarrow (1/2)LiCoO_2 + (1/6)Co_3O_4 + (1/5)CO_2 + (2/15)H_2O \quad (16)$$

or

$$Li_{0.5}CoO_2 + (1/10)C_3H_4O_3 \rightarrow (1/2)LiCoO_2 + (1/2)CoO + (3/10)CO_2 + (1/5)H_2O \quad (17)$$

depending on the different reduction products of $Li_{0.5}CoO_2$. The reaction enthalpies of reactions 16 and 17 are calculated to be -0.982 and -1.375 eV per formula of $Li_{0.5}CoO_2$, which is -1004 J/g and -1406 J/g, respectively, on the basis of the weight of $Li_{0.5}CoO_2$. Reactions 16 and 17 generate a different amount of heat due to the different amounts of oxygen gas released by the decomposition reactions of $Li_{0.5}CoO_2$. These calculated numbers of reaction heats are in good agreement with the experimental value of 1000 ± 250 J/g, reported by Baba et al.[34] These reaction heats are substantially larger than the reaction heat for the exothermic decomposition of $Li_{0.5}CoO_2$ without the presence of electrolyte and can cause the thermal runaway reactions inside the cells.

4. Discussion

Significant thermodynamic instabilities exist for charged electrode materials. The instability of delithiated layered and orthorhombic $LiMO_2$ (M = Ni, Co, and Mn) structures toward spinel formation was already previously pointed out.[13,35] This exothermic reaction can essentially proceed without changes in oxidation state of the cations and is unrelated to the reductive stability of the transition-metal cation. Whether the layered-to-spinel structural conversions occur depends on the kinetics of the cation diffusion. Mn^{3+} and Co^{3+} are known to have the highest and lowest mobility, respectively, among the three cations.[12] Thus, it is more difficult for layered Li_xCoO_2 to complete the conversion into a spinel structure. If the kinetic limitation of the layered-to-spinel transformation at low temperature inhibits the appearance of the intermediate spinel phase, a direct degradation of the layered structure into lower-valence transition-metal oxides occurs, accompanied by the loss of oxygen. The overall reaction then consists of the exothermic layered-to-spinel conversion followed by the endothermic spinel decomposition. The possibility of metal reduction in charged electrodes by the transfer of metal ion to anode was previously suggested,[62] though diffusion of the transition-metal ion through the solid state and through the electrolyte makes this difficult. Metal reduction by loss of oxygen on the cathode side, as modeled in this paper, is a more likely reduction mechanism. We find that the reaction heat for the overall degradation (layered to lower-valence products) can change from positive to negative as the amount of oxygen released increases. Reflecting the different oxidation/reduction potentials of the different M^{4+} ions, the LiM_2O_4 spinels have very different decomposition enthalpies for M = Ni, Co, and Mn. The decomposition of spinel $LiMn_2O_4$ is highly endothermic, about 0.984 eV per formula unit of $LiMn_2O_4$ if it decomposes into orthorhombic $LiMnO_2$ and tetragonal Mn_3O_4. This reaction heat is considerably larger than the numbers for $LiNi_2O_4$ and $LiCo_2O_4$, 0.218 and 0.19 eV, respectively. Under thermodynamic control, the large and positive reaction enthalpy indicates that a relatively high temperature is needed for the decomposition of spinel $LiMn_2O_4$. As the thermodynamic transition temperatures for the $LiNi_2O_4$ and $LiCo_2O_4$ spinels are rather low, their transitions may be kinetically limited.

The three systems have different decomposition products as temperature increases. This is particularly relevant for $x < 0.5$ in Li_xMO_2: from the calculated phase diagram, layered Li_xNiO_2 is located in the $O_2-NiO-LiNi_2O_4$ (or $O_2-NiO-LiNiO_2$ at high temperature) equilibrium triangle; it thus tends to degrade into rocksalt NiO with a loss of oxygen. For layered Li_xCoO_2, the presence of Co_3O_4 in the phase diagram gives decomposition products of spinel Co_3O_4 and O_2, and less oxygen is generated compared to the case of layered Li_xNiO_2. The delithiation of spinel $LiMn_2O_4$ proceeds along the $LiMn_2O_4-(\lambda)Mn_2O_4$ equilibrium line without any loss of oxygen, reflecting again the fact that Mn reaches the 4+ oxidation state more easily than Co or Ni.[63] The fact that it has both a thermodynamically very stable charged and discharged state gives the delithiated spinel $Li_xMn_2O_4$ more thermal stability compared to layered Li_xNiO_2 and Li_xCoO_2.

At elevated temperature, the loss of oxygen for layered Li_xMO_2 brings safety issues for batteries because the released

(62) Ceder, G.; Aydinol, M. K. *Solid State Ionics* **1998**, *109*, 151−157.
(63) Whittingham, M. S. *Chem. Rev.* **2004**, *104*, 4271−4301.

oxygen can react with the organic electrolyte inside the cell. Our study shows that the critical oxygen chemical potential needed to make the combustion of ethylene carbonate thermodynamically favorable is always below the critical oxygen chemical potentials for the decomposition reactions of cathode materials. Thus, the surface reduction of cathode materials by electrolyte is thermodynamically possible. If we assume that the flash point of the electrolyte is the minimum temperature needed to start the reaction between O_2 and the electrolyte, then the bulk combustion will start at the flash point or at the temperature at which oxygen is released from the cathode material, whichever is greater. The heat of electrolyte combustion is 1 order of magnitude larger than those from the exothermic reactions of cathode materials. Even though the oxygen-release reactions from the cathode are endothermic, the combustion of electrolyte by the released O_2 is highly exothermic, making the overall reaction exothermic. As a result, the amount of heat generation depends almost linearly on the amount of oxygen consumed by the electrolyte if excess electrolyte is assumed. This suggests that in the presence of excess electrolyte, layered Li_xNiO_2 can be more dangerous than Li_xCoO_2 as it generates more oxygen gas. On the contrary, spinel $LiMn_2O_4$ is less reactive compared to the layered Li_xMO_2, because the delithiation can proceed without the loss of oxygen. Our result underscores the critical role that nonflammable electrolytes can play in the safety of Li-ion batteries.[64] The cathode decomposition is either mildly exothermic or endothermic (when O_2 is released), which in itself is less likely to lead to a runaway reaction. Only when the released O_2 finds a combustible reagent such as the electrolyte or anode do strongly exothermic reactions occur.

In the present first-principles approach, the GGA+*U* method is crucial to understanding the decomposition mechanisms and obtaining accurate oxidation energies, particularly when the transition-metal ion has an overall change in oxidation state. In some cases, the GGA approximation (without *U*) can give qualitatively incorrect reaction energies, and predict an exothermic reaction to be endothermic (e.g., decomposition of layered $Li_{0.25}CoO_2$, $Li_{0.5}CoO_2$, and $Li_{0.25}NiO_2$). The major uncertainty of the GGA+*U* method is the *U* parameter. In this study, we used *U* values self-consistently calculated in similar crystal structures.[8] *U* parameters determined in this way can give accurate reaction energies for most of the cases in this work, but if a reaction produces a large change in the valence state of transition-metal ions or a dramatic change in crystal structure, the selection of reasonable *U* values can be difficult. The decomposition of spinel $LiNi_2O_4$ to NiO serves as an example. This reaction has half of the Ni reduced from 4+ to 2+. Fitting the calculated formation energy of $LiNiO_2$ ($2Li_2O + 4NiO + O_2 \rightarrow LiNiO_2$) to the experimental value,[65] we obtain a *U* value of 5.2 eV. A decrease of *U* from 6 (used in this work) to 5.2 eV will increase the estimated decomposition temperature in Figure 5a from 220 to 430 K. The latter temperature may be more reasonable, because the presence of spinel $LiNi_2O_4$ as an intermediate phase has been reported in thermal stability tests of layered Li_xNiO_2.[26,27,66,67] Quantitative prediction of thermal decomposition temperatures for some reactions is still a challenge.

The new approach presented in this work is promising for predicting the thermal stability of charged cathode materials. We believe that this first-principles approach can be useful to better understand the decomposition mechanisms of cathode materials and we hope that it will contribute to the development of safe and stable electrode materials.

Acknowledgment. This work was supported by the U.S. Department of Energy under Contract DE-FG02-96ER45571 and the BATT program under Contract 6517748. We thank Jeff Dahn for suggestions to include the electrolyte combustion.

CM0620943

(64) Xu, K.; Zhang, S.; Allen, J. L.; Jow, T. R. *J. Electrochem. Soc.* **2002**, *149*, A1079−A1082.

(65) Wang, M.; Navrotsky, A. *Solid State Ionics* **2005**, *166*, 167−173.

(66) Lee, K. K.; Yoon, W. S.; Kim, K. B.; Lee, K. Y.; Hong, S. T. *J. Electrochem. Soc.* **2001**, *148*, A716−A722.

(67) Lee, K. K.; Yoon, W. S.; Kim, K. B. *J. Electrochem. Soc.* **2001**, *148*, A1164−A1170.

(68) Kang, K.; Chen, C. H.; Hwang, B. J.; Ceder, G. *Chem. Mater.* **2004**, *16*, 2685−2690.